

Nano-structured Electrode Materials with Reduced Amount of Platinum Aimed for Hydrogen Evolution. Part II: Effect of MWCNTs modification

Ana Tomova, Perica Paunović

Faculty of Technology and Metallurgy, University Ss Cyril and Methodius in Skopje, North Macedonia¹
pericap@tmf.ukim.edu.mk

Abstract: Direct Metal Laser Sintering (DMLS) is a revolutionary technology that allows a production of fully functional metal parts directly from a 3D CAD data, eliminating the investment to production tools and technologies which brings considerable cost and time savings. Metal parts made by DMLS technology are fully comparable with casted or machined parts. A range of application of DMLS technologies is very wide – from prototypes, through short-run production to final products. Advantages of DMLS technology are arising along with complexity of parts – more complex geometry of parts (in terms of shape and occurrence of the detail) make DMLS technology even more economically effective.

Keywords: HYDROGEN ECONOMY, CATALYST SUPPORT, MWCNTs MODIFICATION, COBALT, PLATINUM

1. Introduction

Living in the time of exhausted and limited reserves of fossil fuels [1], the “hydrogen economy” is emerging as a promising future energy supply system instead of the existing one based on fossil fuels [2]. The main focus of the hydrogen economy’s activities is directed to selection and development of the effective electrode materials for electrochemical devices for hydrogen production and its conversion to electricity. The modern electrodes materials are consisted of electrocatalytic phase (mainly metals, mixture of metals or mixture of metals and its compounds) and catalyst support (nano-dimensional carbon materials) [1]. The most used traditional electrode material contains platinum nanoparticles deposited on carbon blacks (Vulcan XC-72). In the first part of this paper series, the actual problems with platinum were explained, as well as the pathways for improvement of electrocatalytic activity of non-platinum metals [3]. Here we will explain the importance of the support materials and pathways for their improvement in order to enhance the electrocatalytic activity of the whole electrode material.

Metallic nanoparticles affinity to agglomerate in larger particles and show very poor dispersion, resulting in deterioration of the surface characteristics. This is a considerable limitation of their use as an electrocatalytic electrode material, in fact, they cannot be used as an electrocatalysts individually. To overcome this drawback, they must be applied to a support material. Therefore, the principal function of the support material is to provide a uniform dispersion of the metallic nanoparticles over the whole surface and to avoid their agglomeration. So, the support material should have superior surface characteristics. The other requirements that have to be assured for better performances of the electrode materials are [1]: *i*) high electrical conductivity. Because of the ratio between support material and metallic catalytic phase of 4–5:1, the support material should provide continuous exchange of electron with reacting ions; *ii*) good chemical and mechanical stability to provide long durability of the electrochemical devices and *iii*) to be “non-inert”, i.e. to provide interaction with metallic (catalytic) phase, which improve the electrochemical activity of the electrode material.

The most used support material in hydrogen economy is carbon black (Vulcan XC-72), as result of its appropriate properties, such as a high degree of ordering, surface characteristics and high electroconductivity [4]. The discovery of carbon nanostructures has attracted great attention to their application as a support material in the hydrogen economy. So, the newer carbonaceous materials such as carbon nanotubes (CNTs) and nanofibers were recognized as a very suitable for this purpose [5-7]. In comparison with Vulcan XC-72, CNTs show the following advantages: *i*) higher electroconductivity in range of 10^3 – 10^4 S·cm⁻¹ vs. 4 S·cm⁻¹ [8]; *ii*) higher specific surface area in range of 200–900 m²·g⁻¹ [8]; *iii*) Vulcan XC-72 possesses micropores smaller than 2 nm, which is not the case with CNTs [8]. This is important for the electrocatalytic purpose, because the fine nanostructured metallic particles can sink into the micropores, reducing the number of three-phase boundary reaction sites; *iv*) higher chemical stability, very important parameter for anodic reactions, where the electrochemical degradation of carbon

materials is shown by carbon graphitization [4]. This can be described by the fact that electrochemical corrosion takes place at the edge planes of graphite, whereas the basal planes are relatively inert. Therefore, a higher corrosion resistance was noticed in materials such as Pt/CNTs which are roll-ups of graphene sheets and possess a long-range order, as compared to Pt supported on carbon blacks which have a turbostratic structure and are composed of a mixture of graphite crystallites and amorphous carbon [9].

Because the manufactured MWCNTs always contain impurities such as amorphous carbon, alkali metal nanoparticles [10,11], a further treatment of carbon nanotubes is needed. The purification means remove of the impurities, while activation means making the surface more reactive as result of increased presence of functional groups. One of the most used purification/activation methods is treatment by nitric acid [6,12]. During purification process, shortening and opening of the MWCNTs occurs, implying more active surface.

The main goal of this research is to enhance the electrocatalytic activity of the Co-Pt based electrode materials through the purification/activation of the manufactured MWCNTs in concentrated nitric acid.

2. Materials and Methods

The first experimental step was a purification/activation of the manufactured MWCNTs (Guangzhou Yorkpoint Energy Company, China) in 28%wt. solution of HNO₃. Ultrapurified and deionized water was used for the preparation of the solution. The dispersed MWCNTs into the solution were stirred by magnetic stirrer (1000 rpm) for 4 h. The suspension full of MWCNTs was filtered by vacuum through a micro-filter. Final drying was performed at 95 °C for 12 h. The structural changes of treated MWCNTs related to the manufactured (non-treated), were studied using thermal analysis (TG/DTG), Raman spectroscopy and TEM microscopy. For thermal analysis a Perkin Elmer Pyris Diamond Thermogravimetric/Differential Thermal Analyzer was used. MWCNTs samples were heated in the temperature range of 25÷1000 °C with a heating rate of 20 °C·min⁻¹, in atmosphere of N₂. Scanning of the Raman spectra was performed using Micro-Raman multichannel spectrometer – Horiba JobinYvon LabRam Infinity (*f* x 10) using 532 nm YAG laser. Transmission electron Microscope JEOL JEM - 200 CX was used for TEM observation.

Surface changes were observed by cyclic voltammetry measuring the values of the double layer capacity [13,14]. The ratio of real versus geometric surface area S_R/S_G , of the electrodes was determined as a quotient of the catalyst’s double layer capacity C_{dl} versus the double layer capacity C_{dl0} of a pure oxide surface.

The preparation and composition of the studied electrode materials was identical as in the first part of this paper series [3]. The structural changes of the samples, was studied by infrared FTIR spectroscopy. The FTIR spectra were recorded using KBr pellets at

room temperature with a Perkin-Elmer System 2000 interferometer. Electrochemical characterization was performed using the same instrumentation line and methods as in the first part of this paper series [3].

3. Results and discussions

The electrocatalytic activity of the studied electrode materials expressed through polarization curves in the plot of current density-overpotential ($i-\eta$), are shown in Fig. 1. Corresponding values of Tafel slopes in the lower and higher current regions, as well as the overpotential at reference current density of $60 \text{ mA}\cdot\text{cm}^{-2}$ are listed in Table 1. The order of activity is the same as in the first part of this paper series: $\text{CoPt}(1:1) > \text{Pt} > \text{CoPt}(4:1):\text{Co}$, and the reason of this order was explained. But, if compare the electrocatalytic activity of each metallic phase with that of each metallic phase deposited on non-treated (manufactured) MWCNTs (presented in previous part), significant improvement can be observed. This comparison is shown in Figures 2 to 5.

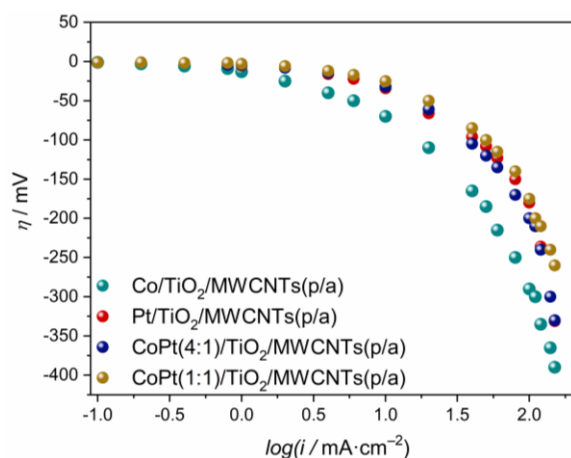


Fig. 1 Polarization curves in the plot $\log i-\eta$ for the studied electrode materials deposited on treated MWCNTs, in 3.5 M KOH

Table 1: Tafel slopes and overpotential at the reference current density of $60 \text{ mA}\cdot\text{cm}^{-2}$ for HE of the studied electrode materials in 3.5 M KOH.

Sample N ^o	Met. phase (10% wt.)	b_1	b_2	η_{60}
1	Pt	23	373	-125
2	CoPt (1:1, wt.)	17	302	-115
3	CoPt (4:1, wt.)	20	365	-135
4	Co	43	383	-215

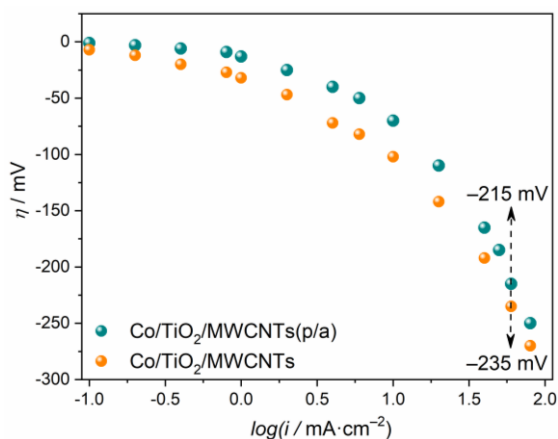


Fig. 2 Polarization curves in the plot $\log i-\eta$ for Co/TiO_2 system deposited on manufactured and treated MWCNTs, in 3.5 M KOH

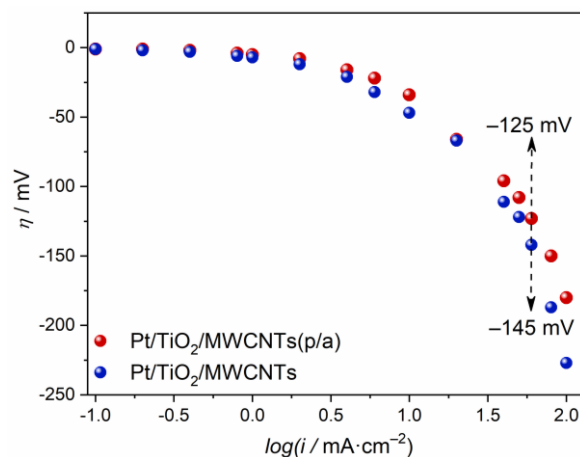


Fig. 3 Polarization curves in the plot $\log i-\eta$ for Pt/TiO_2 system deposited on manufactured and treated MWCNTs, in 3.5 M KOH

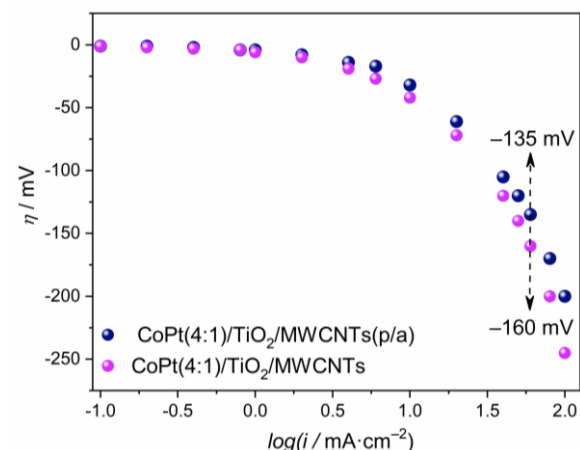


Fig. 4 Polarization curves in the plot $\log i-\eta$ for $\text{CoPt}(4:1)/\text{TiO}_2$ system deposited on manufactured and treated MWCNTs, in 3.5 M KOH

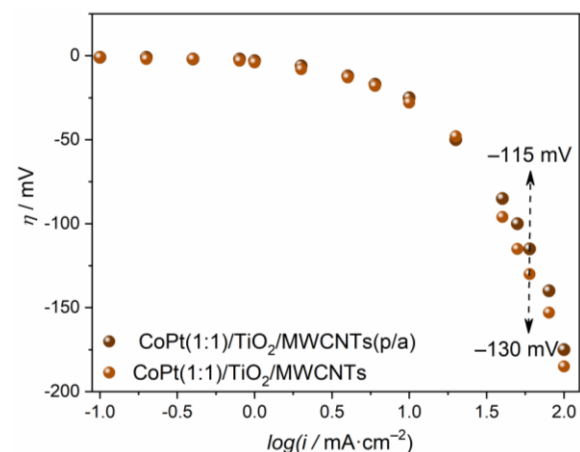


Fig. 5 Polarization curves in the plot $\log i-\eta$ for $\text{CoPt}(1:1)/\text{TiO}_2$ system deposited on manufactured and treated MWCNTs, in 3.5 M KOH

Confirmation of this improvement of electrocatalytic activities of the studied electrode materials are the values of Tafel slopes shown in Table 1 and in Table 2 in the first part of this paper series [3].

To check for some changes in the hypo-hyper d-interaction between the metallic phase and TiO_2 , as result of the MWCNTs treatment, FTIR spectra (Fig. 6) were recorded. All electrode systems show similar spectra and can be concluded that there is not additional hypo-hyper d-interaction as result of MWCNTs treatment. Therefore, the reason for improvement of the electrocatalytic activ-

ity should be sought in the structural or surface changes of MWCNTs as result of their treatment in nitric acid.

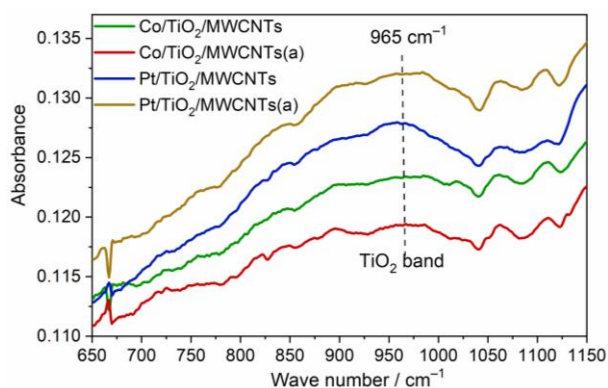


Fig. 6 FTIR spectra for electrode materials with pure metallic phase

Thermal analysis (TG/DTG) of the studied electrode materials has shown that the acid treatment caused higher thermal stability of the MWCNTs. In the DTG spectra shown in Fig. 7, one can see that all characteristic temperatures for the treated MWCNTs are shifted to the higher values. The DTG peak at 573 °C for non-treated MWCNTs is ascribed to the combustion temperature of amorphous carbon, while the peak at 757 °C corresponds to the combustion temperature of the MWCNTs. The corresponding combustion temperatures of amorphous carbon and MWCNTs for acid treated MWCNTs are 641 °C and 893 °C. According to the TG values of temperature shown in Table 2, weight loss of the non-treated MWCNTs starts at 523 °C, with complete oxidation at 617 °C. The corresponding temperatures for acid treated MWCNTs are higher – 585 °C and 847 °C respectively.

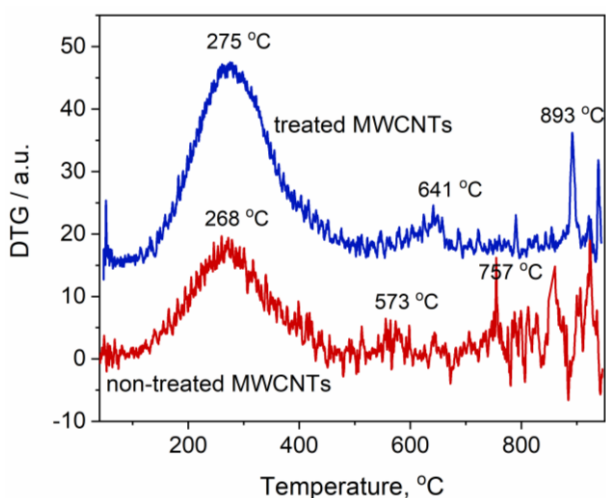


Fig. 7 DTG spectra of non-treated and treated MWCNTs

Table 2: Characteristic TG oxidation temperatures for the non-treated and treated MWCNTs.

Sample	TG ₁	TG ₂	TG ₃
Non-treated MWCNTs	173	523	617
Acid treated MWCNTs	180	585	847

The Raman spectra of the non-treated and purified/activated MWCNTs shown in Fig. 8 are consisted of two well pronounced peaks D and G. D peak at near 1350 cm⁻¹ expressing the presence of disordered carbon structure: defects such as pentagons or heptagons in graphite, vacancies from single to multiple, edges of the graphite crystal, amorphous carbon etc. [15]. G peak at 1585 cm⁻¹ is attributed to the highly oriented graphite [16]. A low pronounced and shouldered peak noted as D' can be observed at position of 1620 cm⁻¹. The presence of the D' peak points out that these carbon nanotubes are multiwalled [17]. The intensity ratio of the characteristic peaks (I_D/I_G) points out on the extent of disorder, i.e. the pro-

nounced presence of defects and impurities in the nanotubes. After the acid treatment of the MWCNTs the value of the I_D/I_G ratio from 1,32 decreases to 1,23. This indicates on the increase of crystallinity of the MWCNTs, i.e. removing of amorphous carbon and reducing the defects within its structure.

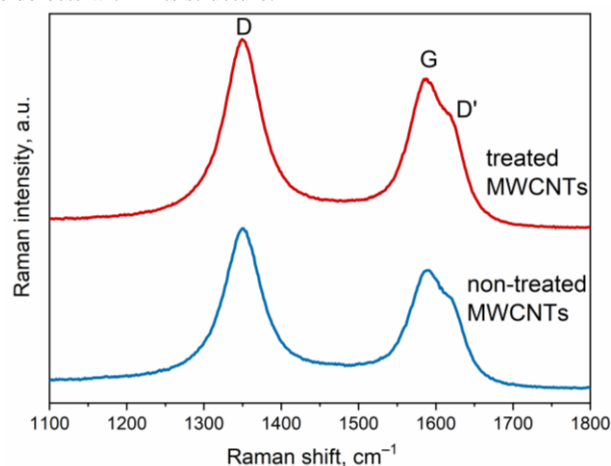


Fig. 8 Raman spectra of non-treated and treated MWCNTs

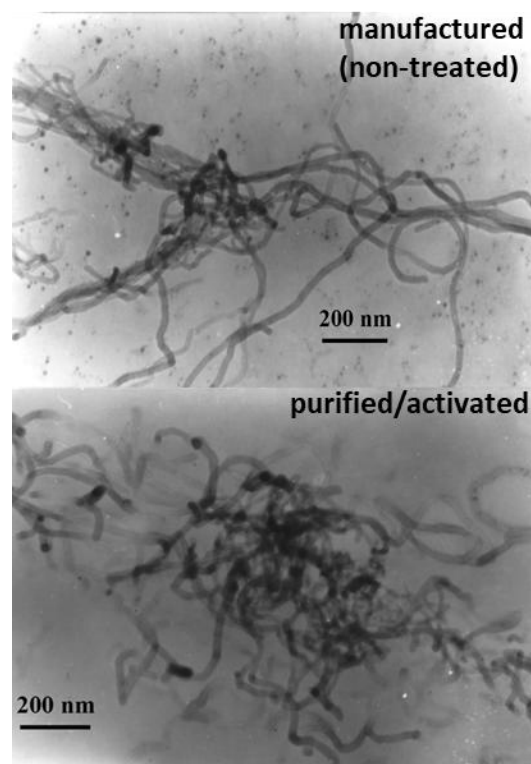


Fig. 9 TEM images of non-treated and treated MWCNTs

From the TEM images shown in Fig. 9, the shortening and opening of the MWCNTs can be clearly seen. This means increase of defects within the MWCNTs structure and increase of the I_D/I_G ratio is expected. But, the Raman results did not show that. The decrease of the I_D/I_G ratio can be explained by the high extent of the removal of amorphous carbon. The shortening and opening of the MWCNTs is an appropriate for electrocatalytic purpose, as result of increased MWCNTs reactivity, facilitating the process of applying the metallic phase over the MWCNTs surface. Also, a higher real surface area of MWCNTs could be expected.

This expectation was confirmed by the values of the double layer capacity for pure carbon phases and the ratio of real vs. geometric surface area (S_R/S_G). The measurements were performed in the region of potentials where only charging of double layer occurs with scanning rate from 1 to 10 mV·s⁻¹. The procedure for determination of C_{dl} for carbon blacks and carbon nanotubes, as well as electrocatalysts deposited on these carbon substrates, is presented elsewhere [18]. The results are shown in Table 3. The acid treated

carbon nanotubes have higher value for the double layer capacity than that of non-treated MWCNTs, i.e. they have more developed surface area expressed with higher ratio of real vs, geometric surface area (S_R/S_G). As was mentioned above, this is result of opening, shortening, and thinning of the nanotubes by HNO_3 treatment. Also, according to the C_{dl} and S_R/S_G values, MWCNTs show almost two times higher surface area than the traditionally used carbon substrate, Vulcan XC-72.

Table 3: Double layer capacity C_{dl} and ratio of real vs. geometrical surface area S_R/S_G for the studied carbon nanostructures.

Sample	C_{dl} , $\text{mF}\cdot\text{cm}^{-2}$	S_R/S_G
Non-treated MWCNTs	331	5520
Acid treated MWCNTs	355	5920
Vulcan XC-72	179	2980

4. Conclusions

According to the presented results, the following conclusions can be drawn:

- During the activation/purification of MWCNTs, two main processes occur: i) removing of other carbonaceous phases such as amorphous carbon and ii) shortening, thinning and opening of the MWCNTs.

- These phenomena favour the increase of the real surface area of the support material (MWCNTs) and consequently of the electrode material as a whole.

- All electrode materials deposited on the acid treated MWCNTs have shown improved electrocatalytic activity related to the corresponding systems deposited on non-treated MWCNTs.

- Compared with traditional electrode material (the same quantity of platinum, 10%wt. deposited on Vulcan XC-72), the best catalytic system 10%CoPt(1:1)/TiO₂/MWCNTs(p/a) has shown much higher electrocatalytic activity (−115 mV vs. −220 mV [19]) at reference current density of 60 mA·cm^{−2}. Even the electrode material with pure Co phase (10%Co/TiO₂/MWCNTs(p/a)) exceeded the electrocatalytic activity of the traditional platinum electrocatalysts (−215 mV vs. −220 mV).

5. References

1. P. Paunović, *Enhancing the Activity of Electrode Materials in Hydrogen Economy*, LAP Lambert Academic Publishing (2018)
2. J. O'M. Bockris, T. N. Veziroglu, D. Smith, *Solar hydrogen energy – the power to save the Earth*, Macdonald Optima, London (1991)
3. P. Paunović, A. Tomova, *this issue*.
4. F. Maillard, P.A. Simonov, E.R. Savinova, in: P. Serp and J. L. Figueiredo (Eds.), *Carbon Materials as Supports for Fuel Cell Electrocatalysts*, John Wiley & Sons (2009)
5. T. Chen, L. Dai, *Mater. Today*, **16**, 271 (2013)
6. P. Serp, M. Corrias, P. Kalck, *Appl. Catal. A: Gen.*, **253**, 337 (2003)
7. U. Sahaym, M. G. Norton, *J. Mater. Sci.*, **43**, 5398 (2008)
8. K. Lee, J. Zhang, H. Wang, P. Wilinson, *J. Appl. Electrochem.*, **36**, 507 (2007)
9. Y. Shao, G. Yin, J. Zhang, Y. Gao, *Electrochim. Acta*, **51**, 5853 (2006)
10. Y. S. Park, Y. C. Choi, K. S. Kim, D. C. Chung, D. J. Bae, K. H. An, S. C. Lim, X. Y. Zhu, Y. H. Lee, *Carbon*, **3**, 655 (2001)
11. D. T. Colbert, J. Zhang, S. M. McClure, P. Nikolaev, Z. Chen, J. H. Hafner, D. W. Owens, P. G. Kotula, C. B. Carter, J. H. Weaver, A. G. Rinzler, R. E. Smalley, *Science*, **266**, 1218 (1994)

12. A. G. Rinzler, J. Liu, H. Dai, P. Nikolaev, C. B. Huffman, F. J. Rodriguez-Macias, P. J. Boul, A. H. Lu, D. Heymann, D. T. Colbert, R. S. Lee, J. E. Fischer, A. M. Rao, P. C. Eklund, R. E. Smalley, *Appl. Phys. A*, **67**, 29 (1998)
13. B. Marsan, N. Fradette, G. Beaudoin, *J. Electrochem. Soc.*, **139**, 1889 (1992)
14. L. M. Da Silva, L. A. De Faria, J. F. C. Boodts, *Electrochim. Acta*, **47**, 395 (2001)
15. H. Hiura, T.W. Ebbesen, J. Fujita, K. Tanigaki, T. Takada, *Nature*, **367**, 148 (1994)
16. F. Tunistra, J. L. Koenig, *Raman Spectrum of Graphite*, *J. Chem. Phys.*, **53**, 1126 (1970)
17. Y. S. Park, Y. C. Choi, K. S. Kim, D. C. Chung, D. J. Bae, K. H. An, S. Ch. Lim, X. Y. Zhu, Y. H. Lee, *Carbon*, **39**, 655 (2001)
18. P. Paunović, A. T. Dimitrov, O. Popovski, D. Slavkov, S. Hadži Jordanov, *Maced. J. Chem. Chem. Eng.*, **26**, 87 (2007)
19. P. Paunović, O. Popovski, A. Dimitrov, D. Slavkov, E. Lefterova and S. Hadži Jordanov, *Electrochim. Acta*, **52**, 4640 (2007)